


# SCIENTIFIC REPORTS



OPEN

## Functional expression of the mechanosensitive PIEZO1 channel in primary endometrial epithelial cells and endometrial organoids

Aurélie Hennes<sup>1,2</sup>, Katharina Held <sup>1,2</sup>, Matteo Boretto<sup>3</sup>, Katrien De Clercq<sup>1,2</sup>, Charlotte Van den Eynde<sup>1,2</sup>, Arne Vanhie<sup>1,4</sup>, Nele Van Ranst<sup>2</sup>, Melissa Benoit<sup>2</sup>, Catherine Luyten<sup>1</sup>, Karen Peeraer<sup>1,4</sup>, Carla Tomassetti<sup>1,4</sup>, Christel Meuleman<sup>1,4</sup>, Thomas Voets<sup>2</sup>, Hugo Vankelecom<sup>3</sup> & Joris Vriens<sup>1</sup>

Successful pregnancy requires the establishment of a complex dialogue between the implanting embryo and the endometrium. Knowledge regarding molecular candidates involved in this early communication process is inadequate due to limited access to primary human endometrial epithelial cells (EEC). Since pseudo-pregnancy in rodents can be induced by mechanical scratching of an appropriately primed uterus, this study aimed to investigate the expression of mechanosensitive ion channels in EEC. Poking of EEC provoked a robust calcium influx and induced an increase in current densities, which could be blocked by an inhibitor of mechanosensitive ion channels. Interestingly, RNA expression studies showed high expression of *PIEZO1* in EEC of mouse and human. Additional analysis provided further evidence for the functional expression of PIEZO1 since stimulation with Yoda1, a chemical agonist of PIEZO1, induced increases in intracellular calcium concentrations and current densities in EEC. Moreover, the ion channel profile of human endometrial organoids (EMO) was validated as a representative model for endometrial epithelial cells. Mechanical and chemical stimulation of EMO induced strong calcium responses supporting the hypothesis of mechanosensitive ion channel expression in endometrial epithelial cells. In conclusion, EEC and EMO functionally express the mechanosensitive PIEZO1 channel that could act as a potential target for the development of novel treatments to further improve successful implantation processes.

Embryo implantation is a fundamental step in reproduction that requires an intimate interaction between a competent blastocyst and a receptive endometrium<sup>1,2</sup>. Active embryo selection at the site of implantation requires the appropriate embryonic signals to be perceived and translated by the endometrium<sup>3</sup>. The current insights into the molecular mechanisms in which chemical and/or physical signals released by the blastocyst and detected by the endometrial epithelial cells (EEC), are still obscure. Ultrastructural animal studies of early stages of implantation have demonstrated a physical interaction between the embryo and the endometrial epithelium<sup>4</sup>. Decidualization, known as the progesterone-dependent differentiation of fibroblast-like endometrial stromal cells into large, secreting decidual cells, is a key step to achieve successful implantation. Interestingly, the decidualization reaction in rodents can be induced in the absence of an embryo by the application of physical signals such as intraluminal injection of oil, or scratching of the endometrium<sup>5</sup>. The signaling role of the endometrial epithelium in processing these physical signals is indispensable since physically stimulated decidualization does not take place when the epithelium is destroyed or removed<sup>6</sup>. In humans, decidualization occurs spontaneously during the luteal phase

<sup>1</sup>Laboratory of Endometrium, Endometriosis & Reproductive Medicine, Department of Development and Regeneration, KU Leuven, Herestraat 49 box 611, 3000, Leuven, Belgium. <sup>2</sup>Laboratory of Ion Channel Research, Department of Cellular and Molecular Medicine, KU Leuven, VIB Center for Brain & Disease Research, Herestraat 49 box 802, 3000, Leuven, Belgium. <sup>3</sup>Laboratory of Tissue Plasticity in Health and Disease, Cluster of Stem Cell and Developmental Biology, Department of Development and Regeneration, KU Leuven, Herestraat 49 box 804, 3000, Leuven, Belgium. <sup>4</sup>Leuven University Fertility Centre, University Hospitals Leuven, Herestraat 49, 3000, Leuven, Belgium. Correspondence and requests for materials should be addressed to J.V. (email: [Joris.Vriens@kuleuven.be](mailto:Joris.Vriens@kuleuven.be))

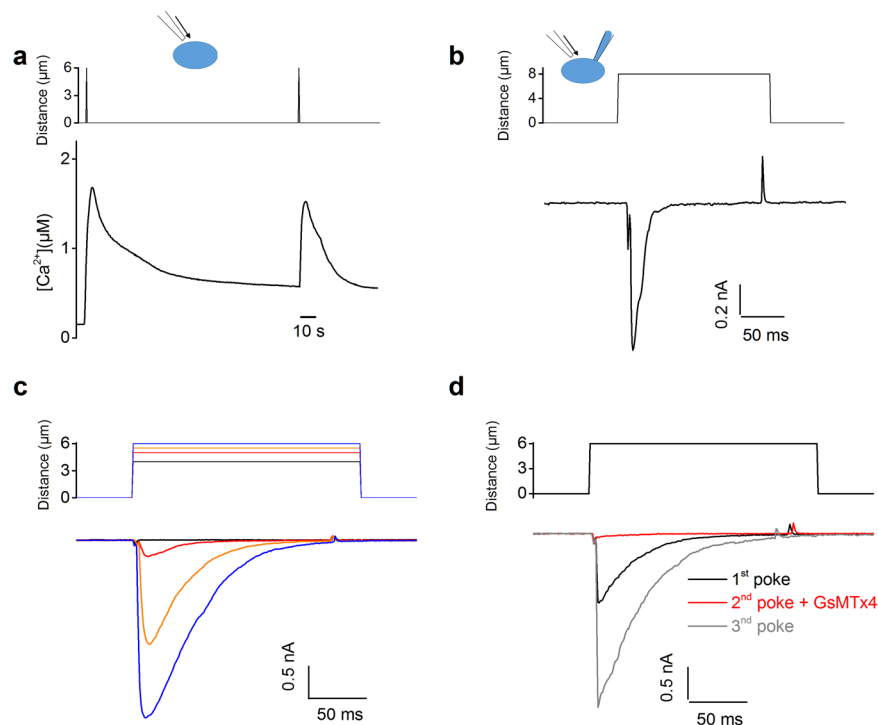


**Figure 1.** Functional expression of a mechanically activated ion channel in primary human EEC. **(a)** Representative trace of ratiometric  $\text{Ca}^{2+}$  imaging (Fura2) on human EEC. Cells were subjected to a series of mechanical stimuli by pressing a glass probe onto the cell surface for 100 ms ( $n = 10$ ). **(b–d)** Mechanically activated currents of hEEC recorded in the whole-cell configuration. **(b)** Representative trace of mechanically activated inward current at  $-60$  mV in hEEC ( $n = 4$ ). **(c)** Representative currents subjected to a series of mechanical steps in  $1 \mu\text{m}$  increments at  $-60$  mV in hEEC. **(d)** Representative traces of mechanically activated currents evoked at  $-60$  mV in the presence of GsMTx4 ( $20 \mu\text{M}$ ).

of the menstrual cycle, in the absence of a blastocyst. However, clinical studies in women with previous repeated *In Vitro* Fertilization (IVF) failure suggest that endometrial injury, before IVF treatment, is associated with increased rates of implantation<sup>7–9</sup>. Nevertheless, the molecular mechanism behind this phenomenon and the involvement of mechanosensitive molecules are yet to be unraveled. Mechanosensitive ion channels are attractive candidates as transducers to transform the physical stimulus into an electrical signal. Earlier studies have reported the epithelial sodium channel (ENaC), a proposed mechanosensor<sup>10,11</sup>, as a regulator of the prostaglandin  $\text{E}_2$  production by the endometrial epithelium, a molecule that is required for embryo implantation<sup>12</sup>. Interestingly, several other ion channels, including the family of PIEZO channels<sup>13</sup>, and the polymodal members of the Transient Receptor Potential (TRP) superfamily, have been described as mechanosensitive<sup>14–23</sup>. PIEZO1 expression is described in lungs, bladder, pancreas and skin, where mechanosensation has important biological roles. However, unlike PIEZO2, which is highly expressed in sensory dorsal root ganglia, PIEZO1 is not expressed in sensory neurons<sup>13</sup>. This study aims to provide evidence for the endogenous expression of mechanosensitive ion channels in EEC of human and mouse.

Ethical and practical considerations often limit the use of primary human endometrial epithelial cells (hEEC) for research purposes. Even more, hEEC have proven difficult to isolate and to culture, resulting in the use of endometrial epithelial cancer cell lines for research. However, their physiological relevance as a model for endometrial epithelial cell can be questioned<sup>24</sup>. Recently, 3D human endometrial organoids (EMO) were demonstrated to represent a valuable model for hEEC, reproducing phenotypical and physiological aspects of the tissue, and can provide an important tool to study the different aspects of implantation<sup>25</sup>. Moreover, the organoids are long-term expandable while retaining their properties, thereby providing a more accessible source of endometrial epithelial cells. Here, we evaluate the potential of EMO as a valid model for primary human EEC to investigate the embryo-uterine crosstalk by studying the functional expression of mechanosensitive ion channels.

## Results

**Mechanosensitivity in human endometrial epithelial cells.** Primary cultures of human EEC (hEEC) were established starting from endometrial biopsies. The matrix-metalloproteinase 2 and 7 (MMP-2 and MMP-7) were used as markers to confirm the epithelial character of the endometrial cells<sup>26</sup>. Typically, hEEC showed low mRNA expression of the stromal marker *MMP-2*, whereas the epithelial marker *MMP-7* was highly expressed. In addition, these results were in line with the positive immunostaining for MMP-7 (Supplementary Fig. S1). Interestingly, mechanical stimulation of hEEC, by poking of the cell membrane, induced a robust and transient  $\text{Ca}^{2+}$  influx (mean  $\Delta\text{Ca}^{2+} = 1315 \pm 335 \text{ nM}$ ) (Fig. 1a). When  $\text{Ca}^{2+}$  was omitted from the extracellular medium

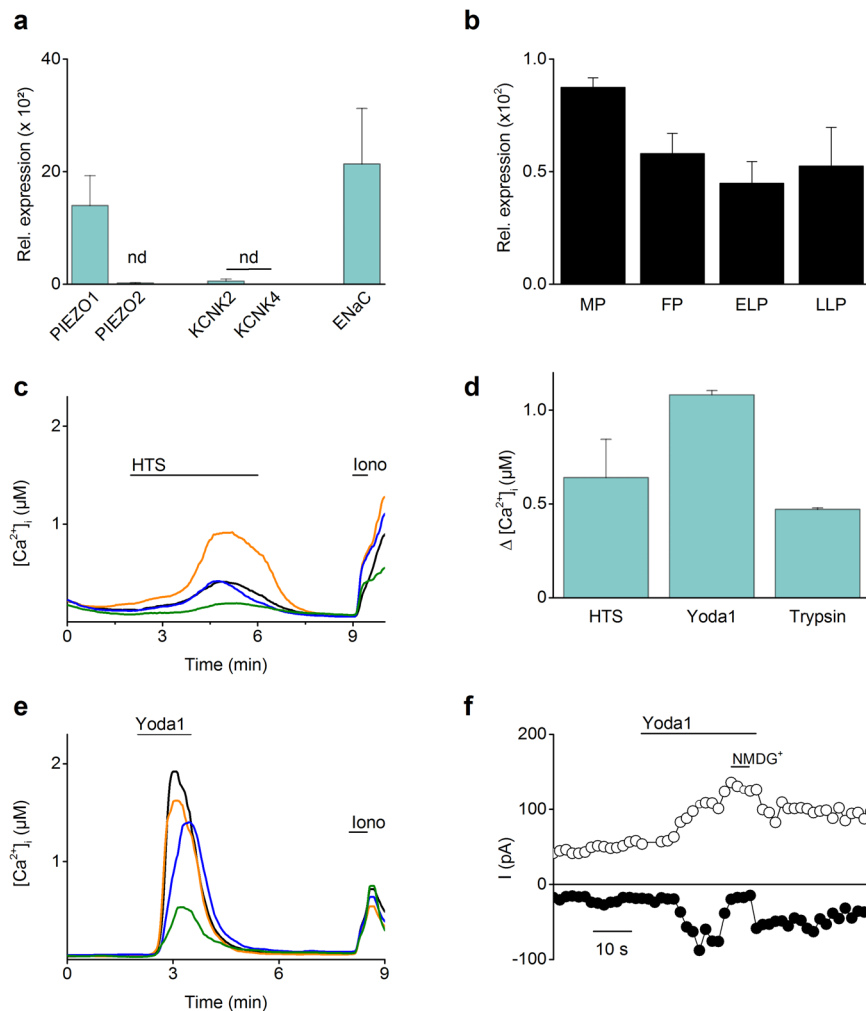


**Figure 2.** Functionality of the mechanosensitive PIEZO1 channel in hEEC. **(a)** mRNA expression levels of mechanosensitive ion channels in primary hEEC. mRNA levels were relatively quantified to the geometric mean of the housekeeping genes *HPRT1* and *PGK1* and represented as mean  $\pm$  SEM.  $n = 4$ , Nd = not detectable. **(b)** RT-qPCR results of *PIEZO1* mRNA expression levels in human biopsies taken at different stages of the menstrual cycle: menstrual phase (MP, days 1–5,  $n = 6$ ), follicular phase (FP, days 6–14,  $n = 21$ ), early luteal phase (ELP, days 15–20,  $n = 15$ ) and late luteal phase (LLP, days 21–28,  $n = 9$ ). **(c–e)** Time course of Ca<sup>2+</sup> experiments in which a hypotonic solution (HTS; 210 mOsm) **(c)** or the PIEZO1 agonist **(e)** was added to hEEC. Shown are four representative traces, at the indicated time points HTS, Yoda1 (5  $\mu$ M) or ionomycin (Iono, 2  $\mu$ M) were added to the cells.  $n = 3$  independent experiments, with a total of minimal 350 cells. Ionomycin was applied at the end of each experiment as a positive control. **(d)** Mean Ca<sup>2+</sup> increase of responding cells to HTS, Yoda1 (5  $\mu$ M) or trypsin (2  $\mu$ g/ml). Amplitudes are represented as mean  $\pm$  SEM. **(f)** Time course at  $\pm 80$  mV of a whole-cell patch clamp recording showing the effect of Yoda1 (10  $\mu$ M) in primary hEEC ( $n = 4$ ). At the indicated period, Na<sup>+</sup> and Ca<sup>2+</sup> were replaced by NMDG<sup>+</sup>.

similar mechanical stimulation of the plasma membrane did not induce any increase in intracellular Ca<sup>2+</sup> concentration. However, application of ionomycin after poking of the cells evoked an increase in intracellular Ca<sup>2+</sup> concentration by depletion of the Ca<sup>2+</sup> stores (Supplementary Fig. S2). Further validation of the functional expression of mechanosensitive ion channels was performed using the whole-cell patch clamp technique in order to measure direct channel activation. Mechanical poking of hEEC induced transient increases in current densities (Fig. 1b) which were rapid (latencies < 1 ms), and voltage dependent (mean current increase =  $572 \pm 22$  pA and  $-915 \pm 22$  pA at +50 mV and -60 mV respectively) and showed a time dependent activation ( $\tau \sim 1.14 \pm 0.43$  ms at -60 mV) and inactivation ( $\tau \sim 22.4 \pm 2.9$  ms at -60 mV). The increase in current density by application of a mechanical stimulus was dependent of the depth of the poking since increased poking distances enlarged the current amplitude (Fig. 1c). Note that a minimal indentation of 5  $\mu$ m was required to induce a current increase (Fig. 1c). The mechanosensitivity of hEEC was fully inhibited in the presence of GsMTx4, a peptide widely used to block mechanically activated channels<sup>27</sup> (Fig. 1d). Altogether, these results demonstrated the endogenous expression of a mechanosensitive ion channel in hEEC.

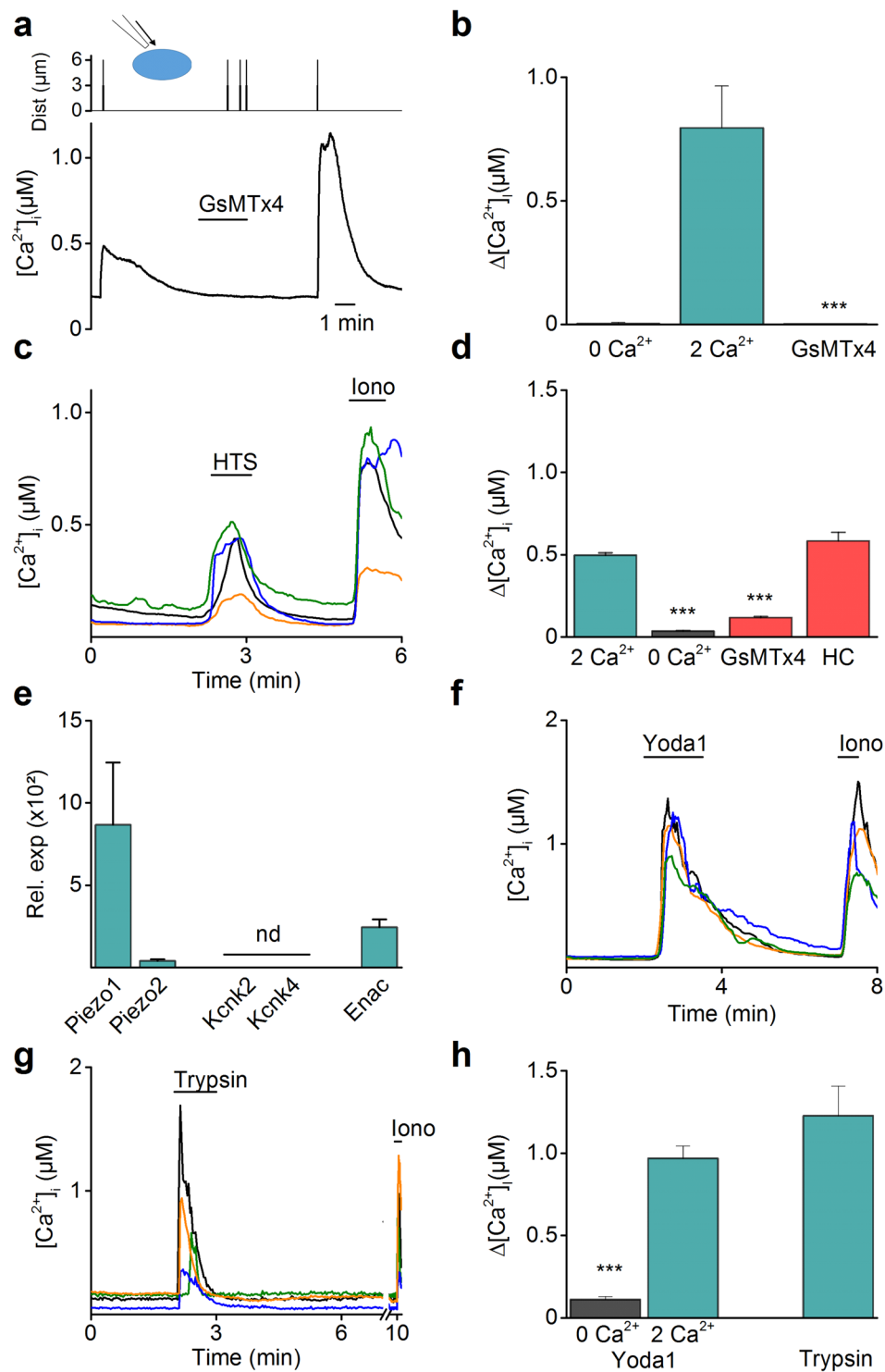


**Figure 3.** Mechanosensitive ion channels in primary EEC of mouse. **(a)** Time course showing the intracellular  $\text{Ca}^{2+}$  concentration of mouse EEC upon mechanical stimulation ( $5\ \mu\text{m}$  for 100 ms) at the indicated time points. When indicated the spider toxin GsMTx4 ( $20\ \mu\text{M}$ ) was added to the external solution ( $n = 12$ ). **(b)** Mean amplitude of  $[\text{Ca}^{2+}]_i$  in mEEC, represented as the difference between the peak value and the baseline value after mechanical poking of the cells in 0 mM extracellular  $\text{Ca}^{2+}$ , 2 mM  $\text{Ca}^{2+}$  and in the presence of the inhibitor GsMTx4 ( $20\ \mu\text{M}$ ). Data are represented as mean  $\pm$  SEM. \*\*\* $p < 0.001$  using the non-parametric Kruskal-Wallis test compared to 2 mM  $\text{Ca}^{2+}$  conditions. **(c)** Example traces of hypotonic (HTS), (210 mOsm) - induced intracellular  $\text{Ca}^{2+}$  change in mEEC.  $N = 3$  independent experiments with a total minimum of 1500 cells. **(d)** Mean amplitude of  $[\text{Ca}^{2+}]_i$  in mEEC, after application of HTS in an extracellular solution containing 0 mM, 2 mM  $\text{Ca}^{2+}$  and in the presence of GsMTx4 ( $20\ \mu\text{M}$ ) or the TRPV4 inhibitor HC-067047 (HC; 100 nM). \*\*\* $p < 0.001$  using the non-parametric Kruskal-Wallis test corrected with Dunn's multiple comparisons to 2 mM  $\text{Ca}^{2+}$  conditions.  $N = 3$  independent experiments with a total minimum of 800 cells. **(e)** mRNA

expression levels of mechanosensitive ion channels in primary mEEC. mRNA levels were relatively quantified to the geometric mean of the housekeeping genes *Tbp* and *Pgk1* and represented as mean  $\pm$  SEM ( $n = 3$ ). Nd = not detectable. (f,g) Depict stimulation of cells with either Yoda1 (5  $\mu$ M) or trypsin (20  $\mu$ g/ml) to induce intracellular  $\text{Ca}^{2+}$  influxes. Ionomycin (Iono, 2  $\mu$ M) was applied at the end of each experiment as a positive control. Each line represents a single cell and four representative traces are shown.  $n = 3$  experiments, with a total of minimum 180 cells per condition. (h) Mean  $\text{Ca}^{2+}$  amplitude of responding cells to Yoda1 (5  $\mu$ M) and trypsin (20  $\mu$ g/ml) in normal medium containing 2 mM external  $\text{Ca}^{2+}$  and  $\text{Ca}^{2+}$  free conditions. Amplitudes are represented as mean  $\pm$  SEM. \*\*\* $p < 0.001$  using the non-parametric Mann-Whitney U test compared to 2 mM  $\text{Ca}^{2+}$  conditions.

**The mechanosensitive PIEZO1 channel is functionally present in human EEC.** To characterize the molecular identity of the mechanosensitive ion channels in hEEC, the expression of candidate mechanosensitive ion channels, including members of the PIEZO family<sup>13</sup> and the two-pore  $\text{K}^+$  (KCNK) family<sup>28,29</sup>, were examined. RT-qPCR experiments showed detectable mRNA expression levels of *PIEZO1* ( $\text{Ct} < 34$ ), while the expression levels of *PIEZO2*, *KCNK2* and *KCNK4* were below the detection level ( $\text{Ct} > 34$ ). As a control, high levels of mRNA expression were detected for the *ENaC* channel, supporting the epithelial character of the cells (Fig. 2a). In addition, gene expression of *PIEZO1* was also detected in human endometrial stromal cells (Supplementary Fig. S3) and in human endometrial biopsies (Fig. 2b). Induced cell swelling via application of a hypotonic solution (HTS) resulted in a  $\text{Ca}^{2+}$  influx in hEEC (mean  $\Delta\text{Ca}^{2+} = 640 \pm 204$  nM) (Fig. 2c,d). Furthermore, application of the selective chemical agonist of the PIEZO1 channel, Yoda1<sup>30</sup>, induced robust increases in intracellular  $\text{Ca}^{2+}$  concentration (mean  $\Delta\text{Ca}^{2+} = 1081 \pm 23$  nM) (Fig. 2d,e). In whole-cell patch clamp experiments, application of Yoda1 evoked an increase in both in- and outwardly rectifying current densities (mean  $\Delta I = -97.9 \pm 50.5$  pA and  $69.8 \pm 29.7$  pA at  $-80$  mV and  $+80$  mV respectively) with an average reversal potential of  $+2.3$  mV (Fig. 2f). To confirm the epithelial character of the cells, functional expression of ENaC was evaluated via stimulation with trypsin, a protease activator of the channel<sup>31</sup>, which resulted in a  $\text{Ca}^{2+}$  influx (mean  $\Delta\text{Ca}^{2+} = 470 \pm 8$  nM) (Fig. 2d) in 98.5% of the cells. Together, these results provide evidence for the endogenous expression of the mechanosensitive PIEZO1 in hEEC.

**Functional expression of mechanosensitive ion channels in mouse EEC.** Similarly, the expression of candidate mechanosensitive ion channels was investigated in primary mouse endometrial epithelial cells (mEEC)<sup>32</sup>. The epithelial character of mEEC was validated by immunostaining for the markers MMP-2 and MMP-7<sup>26</sup> (Supplementary Fig. S4). Next, mechanical poking of mEEC resulted in a rapid and reversible  $\text{Ca}^{2+}$  influx (mean  $\Delta\text{Ca}^{2+} = 795 \pm 169$  nM) (Fig. 3a,b). However, when  $\text{Ca}^{2+}$  was omitted from the extracellular medium, mechanical stimulation of the cell membrane did not induce any  $\text{Ca}^{2+}$  influx (mean  $\Delta\text{Ca}^{2+} = 2 \pm 4$  nM) (Fig. 3b). Similar to hEEC, incubation by GsMTx4 induced a full block (100%) of the mechanically evoked  $\text{Ca}^{2+}$  influx (Fig. 3a,b). Moreover, application of a hypotonic solution (HTS) resulted in an increase in  $\text{Ca}^{2+}$  concentration (mean  $\Delta\text{Ca}^{2+} = 496 \pm 15$  nM) (Fig. 3c) which was strongly reduced in the absence of extracellular  $\text{Ca}^{2+}$  (mean  $\Delta\text{Ca}^{2+} = 36 \pm 3$  nM) in mEEC. The HTS-induced  $\text{Ca}^{2+}$  influx was significantly blocked in the presence of GsMTx4 (mean  $\Delta\text{Ca}^{2+} = 118 \pm 6$  nM) while incubation with the TRPV4 antagonist HC-067047<sup>33</sup> (HC) was without effect on the HTS-induced  $\text{Ca}^{2+}$  influx (mean  $\Delta\text{Ca}^{2+} = 583 \pm 53$  nM) (Fig. 3d).

RT-qPCR experiments on mEEC displayed detectable mRNA expression of *Piezo1* and *Enac* channels ( $\text{Ct} < 34$ ), while no gene expression was detected for *Piezo2*, *Kcnk2* and *Kcnk4* ( $\text{Ct} > 34$ ) (Fig. 3e). Detectable mRNA levels for *Piezo1* were also observed in mouse endometrial stromal cells (mESC) (Supplementary Fig. S3). Moreover, poking of the plasma membrane of mouse PIEZO1 (mPIEZO1) overexpressing HEK-293T cells induced a transient  $\text{Ca}^{2+}$  influx (mean  $\Delta\text{Ca}^{2+} = 918 \pm 109$  nM) which was comparable to the  $\text{Ca}^{2+}$  influx in mEEC after poking of the cell (Supplementary Fig. S5). In contrast, application of the poking protocol to non-transfected HEK-293T cells did not induce any increase in intracellular  $\text{Ca}^{2+}$  (mean  $\Delta\text{Ca}^{2+} = 7 \pm 2$  nM). PIEZO1 overexpressing cells showed an increase in current density after poking of the cell membrane in whole cell patch clamp experiments, exhibiting a similar time dependent activation and inactivation as in hEEC<sup>34</sup> ( $\tau \sim 2.34$  ms and  $\tau \sim 8.67$  ms for activation and inactivation respectively) (Supplementary Fig. S5). In addition, stimulation of mEEC by Yoda1 produced a reversible rise in intracellular  $\text{Ca}^{2+}$  (mean  $\Delta\text{Ca}^{2+} = 968 \pm 75$  nM) (Fig. 3f,h). The percentage of Yoda1 responders and the amplitude of the  $\text{Ca}^{2+}$  influx were significantly reduced when  $\text{Ca}^{2+}$  was omitted from the extracellular solution (only 4.8% responders, mean  $\Delta\text{Ca}^{2+} = 110 \pm 17$  nM) (Fig. 3h). Similar results were observed in HEK-293T cells overexpressing mPIEZO1, which showed strong  $\text{Ca}^{2+}$  increases after Yoda1-stimulation (mean  $\Delta\text{Ca}^{2+} = 570 \pm 56$  nM) whereas only 2.5% of non-transfected cells showed responses to Yoda1, with significantly reduced  $\text{Ca}^{2+}$  influx ( $p < 0.001$ ) (mean  $\Delta\text{Ca}^{2+} = 132 \pm 6$  nM) compared to mPIEZO1 transfected cells (Supplementary Fig. S5). Furthermore, stimulation of mEEC with trypsin induced a strong  $\text{Ca}^{2+}$  influx ( $\Delta\text{Ca}^{2+} = 1227 \pm 179$  nM) in 56.7% of the cells (Fig. 3g,h), which was comparable to earlier reports showing the trypsin-induced calcium influxes in mouse endometrial cells<sup>12</sup> and validates the epithelial character of the investigated cells.

Interestingly, *in situ* hybridisation (RNAscope) for *Piezo1* in sections of the uterine horn revealed a prominent signal for *Piezo1* RNA in luminal epithelial cells, while the fluorescent signal intensity in the stromal part was lower (Fig. 4). The specificity of the RNA probes was evaluated in bladder urothelium<sup>35</sup> and trigeminal neurons<sup>13</sup> as positive and negative control tissue, respectively (Supplementary Fig. S6). To validate the expression of *Piezo1* RNA in the epithelial cells, *in situ* hybridisation for *Trpv6* was tested, showing positive *Trpv6* signals, exclusively in the luminal and glandular epithelial cells of the uterine horn. These results are in line with earlier reports showing typical TRPV6 expression in the endometrial epithelial cells of the mouse<sup>36</sup>. Merging both *Piezo1* and *Trpv6*



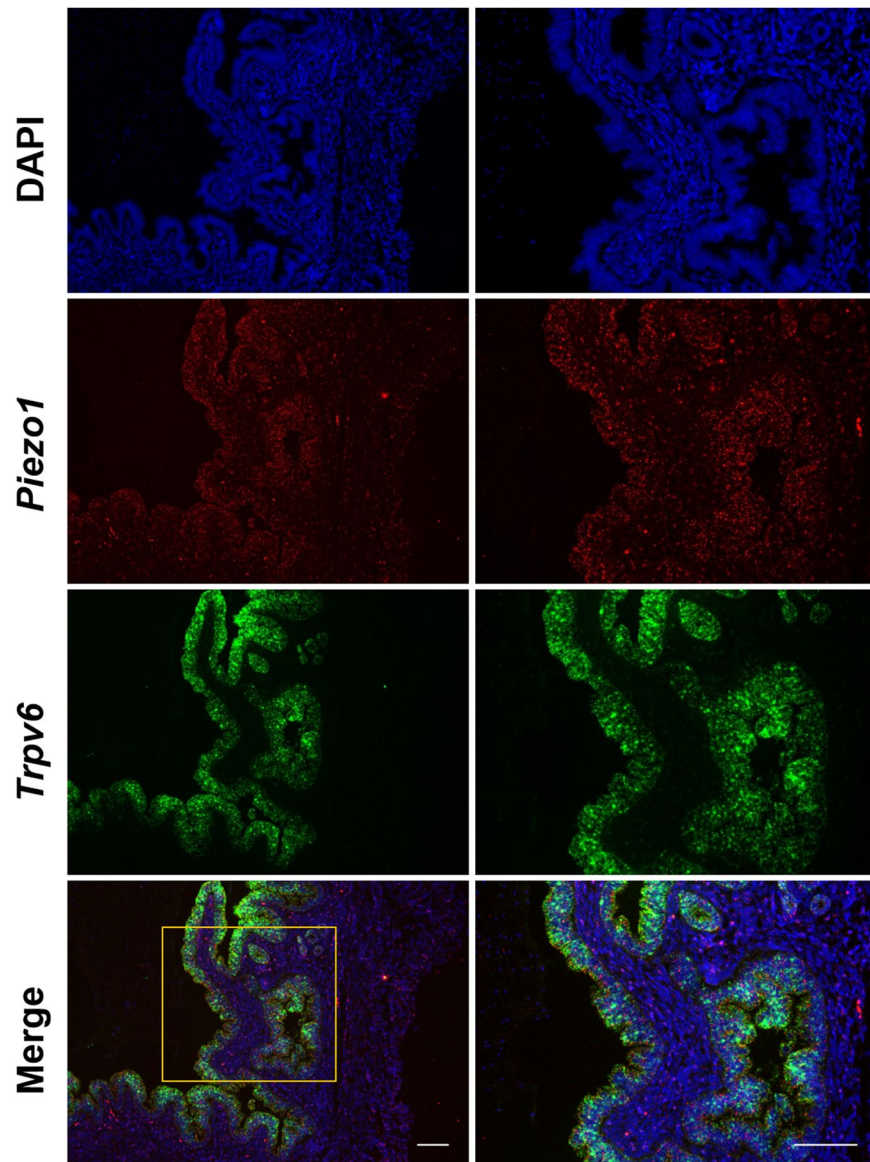


**Figure 4.** *In Situ* hybridization showing *Piezo1* mRNA expression in endometrial epithelial cells. *In situ* hybridization (ISH) on paraffin section from the uterine horn. The bottom panel shows the merged image obtained from DAPI (blue), *Piezo1* (red) and *Trpv6* (green color) stainings. Right panels are magnification of a specific region shown in the left image. Pictures were taken using a 10x objective. Scale bar: 100  $\mu\text{m}$ .

signals, resulted in a positive staining for both channels in the endometrial epithelial cells. Taken together, these experiments provide evidence for the expression of PIEZO1 in endometrial epithelial cells of the mouse.

**TRP channels in human EEC.** In earlier reports, several polymodal members of the TRP superfamily were proposed as candidates involved in sensing mechanical forces<sup>37</sup>. Therefore, hEEC were evaluated for the gene expression pattern of a selected number of TRP channels based on earlier expression studies performed on human endometrial biopsies<sup>38</sup>. RT-qPCR experiments showed detectable mRNA expression levels of *TRPV1*, *TRPV2*, *TRPV4*, *TRPV6*, *TRPC1*, *TRPC4*, *TRPC6*, *TRPM4* and *TRPM7* (Ct values < 34), with *TRPV6*, *TRPM4* and *TRPM7* showing the highest expression levels. In contrast, expression levels for *TRPA1*, *TRPC3*, *TRPC5*, *TRPC7*, *TRPM1*, *TRPM2*, *TRPM3*, *TRPM5*, *TRPM6* and *TRPM8* were below detection limit (Ct values  $\geq 34$ ) (Supplementary Fig. 7). Next, the functional expression of these TRP channels was tested using  $\text{Ca}^{2+}$  microfluorimetry experiments (Supplementary Fig. 7). As specific TRP channel pharmacology is scarce, only a limited number of TRP channels could be tested. Cells were stimulated with  $\Delta^9$ -tetrahydrocannabinol (THC), GSK1016790A (GSK), 1-oleoyl-2-acetyl-glycerol (OAG), (–) Englerin A (EA) or mibefradil (Mib) to assess the functionality of TRPV2, TRPV4, TRPC6, TRPC1/C4 heteromultimers, or TRPM7 respectively. A significant calcium response was observed upon stimulation of hEEC with the TRPM7 agonist mibefradil<sup>39</sup> (mean  $\Delta\text{Ca}^{2+} = 1038 \pm 58 \text{ nM}$ ) (Fig. 5g and Supplementary Fig. 7). However, none of the other TRP channel agonists

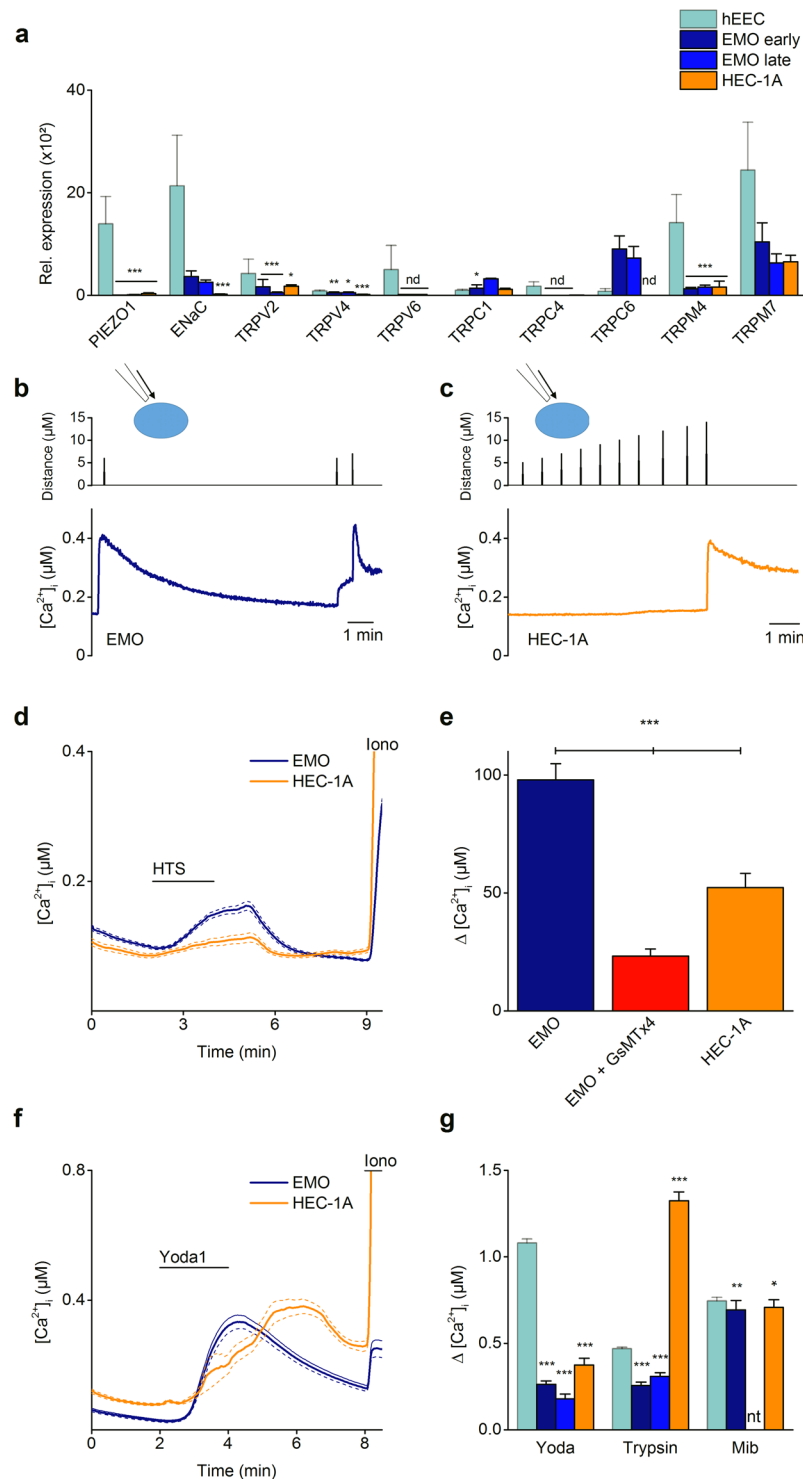


**Figure 5.** EMO as a model for human endometrial epithelial cells. **(a)** mRNA expression levels of selected ion channels in primary hEEC (light blue), early (P2) (blue) and late (P8) (dark blue) passage EMO, and the endometrial epithelial cell line HEC-1A (orange). mRNA levels were relatively quantified to the geometric mean of the housekeeping genes *HPRT1* and *PGK1* and represented as mean  $\pm$  SEM.  $n = 4$  (hEEC),  $n = 3$  (EMO). \* $p < 0.05$ , \*\* $p < 0.01$  compared to the hEEC condition with Two-way Anova and Dunnett's multiple comparison test; Nd = not detectable. **(b–g)** Ca<sup>2+</sup> microfluorimetry. Representative trace of ratiometric Ca<sup>2+</sup> imaging (Fura2) on EMO **(b)** and HEC-1A **(c)**. Cells were subjected to a series of mechanical stimuli by pressing a glass probe onto the cell surface for 100 ms ( $N \geq 10$  independent experiments). **(d)** Time course of Ca<sup>2+</sup> experiments in which a hypotonic solution (HTS; 210 mOsm) was added to either EMO or HEC-1A cells at the indicated time point. Ionomycin (Iono; 2  $\mu$ M) was applied as a positive control. Shown is the mean trace  $\pm$  SEM. The corresponding mean amplitude of [Ca<sup>2+</sup>]<sub>i</sub> upon application of HTS in either 2 mM extracellular Ca<sup>2+</sup> or in the presence of GsMTx4 (20  $\mu$ M) is shown in **(e)**. \*\*\* $p < 0.001$  using the non-parametric Kruskal-Wallis test

corrected with Dunn's multiple comparisons.  $n = 3$  experiments with a total minimum of 200 cells. (f) Time course of intracellular  $\text{Ca}^{2+}$  in EMO and HEC-1A upon stimulation with Yoda1 (5  $\mu\text{M}$ ). Ionomycin (Iono; 2  $\mu\text{M}$ ) was applied as a positive control. Shown is the mean trace  $\pm$  SEM. (g) represents the mean amplitude of  $[\text{Ca}^{2+}]_i$  upon application of Yoda1, trypsin or mibefradil (mib) in either hEEC, early passage EMO, late passage EMO or HEC-1A cells. \* $p < 0.05$ , \*\* $p < 0.01$ , \*\*\* $p < 0.001$  using the non-parametric Kruskal-Wallis test corrected with Dunn's multiple comparisons compared to the hEEC conditions.  $n = 3$  experiments with a total minimum of 80 cells. nt = not tested.

induced a significant increase in calcium concentration in hEEC (% of responding cells  $\leq 2$ ). Altogether, these results showed functional expression of TRPM7, while no functional expression was detected for TRPV2/V4 and TRPC1/C4/C6 in human endometrial epithelial cells, excluding the potential contribution of polymodal TRP channels in the mechanosensitivity of hEEC.

**Endometrial organoids as a model to investigate ion channel activity.** Acquiring sufficient material for the culture of human endometrial epithelial cells is often bound to ethical and practical issues, and provides a challenge in terms of long-term culture. Popular endometrial epithelial cell lines are derived from cancers and do not fully mimic the cellular background of the inner layer of the uterine wall. Recently, a new tool emerged, i.e. endometrial epithelium organoids<sup>25,40</sup>. As organoid epithelial cells are derived from identical starting material as primary hEEC, their physiology may be more closely related to primary cells as compared to the available endometrial epithelial cancer cell lines. To validate whether endometrial organoids relate to primary hEEC in terms of ion channel functionality, the expression pattern of several channels was investigated. To start, organoids were dissociated into single cells and seeded as a monolayer, thereby revealing a morphology comparable to hEEC. After validating the epithelial character of EMO-derived cells (Supplementary Fig. S8), the expression of mechanosensitive ion channels and TRP channels was evaluated in early passage (P2) intact endometrial organoids (EMO). Surprisingly, gene expression of *PIEZO1* was undetected ( $\text{Ct} > 35$ ), whereas gene expression of *ENAC* was observed ( $\text{Ct} < 34$ ) in the intact EMO, albeit at a significantly lower level (Fig. 5a). However, RT-qPCR results from 2D and 3D cultures of organoids showed increased *PIEZO1* RNA expression upon 2D culture conditions (Supplementary Fig. S9), indicating potential alterations in gene expression induced by differences in culture conditions. In addition, the expression pattern of TRP channels in EMO was similar compared to hEEC ( $\text{Ct} < 34$ ), although most levels of expression tended to be lower. Nevertheless, a positive correlation was shown for the TRP channel expression levels comparing hEEC and EMO (Spearman correlation = 0.66;  $p < 0.05$ ) (Supplementary Fig. 7).

As long-term expandability represents an important asset of organoids, expression of a selected panel of ion channels was tested after long-term culture (Passage (P) 8). RT-qPCR analysis showed a steady expression profile for all of the examined channels as compared to early (P2) passage EMO (Fig. 5a).

Mechanical stimulation of 2D cultures of EMO induced  $\text{Ca}^{2+}$  influxes after poking of the cell membrane or application of a hypotonic solution (mean  $\Delta\text{Ca}^{2+} = 98 \pm 7$  nM). The HTS-induced increase in intracellular  $\text{Ca}^{2+}$  was significantly reduced in the presence of GsMTx4 (Fig. 5b,d,e). Moreover, ligand activation of *PIEZO1* evoked a  $\text{Ca}^{2+}$  influx in early and late passage (P8) EMO (mean  $\Delta\text{Ca}^{2+} = 262 \pm 19$  nM and  $179 \pm 28$  nM for P2 and P8 respectively). However, the mean amplitude of the  $\text{Ca}^{2+}$  influx after mechanical and chemical stimulation of EMO was lower as compared to hEEC (Fig. 5g). Stimulation of EMO derived cells with TRP channel agonists (EA, GSK, OAG and THC) did not induced a significant calcium influx, while robust responses were detected after application of mibefradil that were somewhat reduced compared to primary hEEC (mean  $\Delta\text{Ca}^{2+} = 745 \pm 21$  nM vs  $694 \pm 54$  nM for hEEC and EMO respectively) (Fig. 5g).

To validate EMO as model for endometrial epithelial cells, analogue experiments were performed on the endometrial cancer cell line HEC-1A<sup>41</sup>. Overall RT-qPCR experiments showed significantly low(-er) gene expression levels in HEC-1A cells for some of the assessed ion channels compared to hEEC (Fig. 5a). Correlation studies showed distinct ion channel expression patterns for hEEC and HEC-1A (Spearman correlation = 0.52;  $p = 0.13$ ) (Supplementary Fig. S10). At the functional level, HEC-1A cells showed calcium responses to mechanical poking of the cell membrane and to application of a hypotonic solution. However, the sensitivity to mechanical stimulation was remarkably lower in HEC-1A cells as the minimal indentation to induce a  $\text{Ca}^{2+}$  response (mean minimal indentation of  $14.6 \pm 3$   $\mu\text{m}$  and  $7.2 \pm 2$   $\mu\text{m}$  for HEC-1A and EMO respectively) and the HTS-induced  $\text{Ca}^{2+}$ -increase were significantly different compared to EMO (mean  $\Delta\text{Ca}^{2+} = 53 \pm 6$  nM for HEC-1A) (Fig. 5c-e). In contrast, calcium responses to Yoda1 (mean  $\Delta\text{Ca}^{2+} = 374 \pm 39$  nM) were comparable to EMO whereas the responses to trypsin stimulation were three times higher in HEC-1A cells (mean  $\Delta\text{Ca}^{2+} = 1325 \pm 50$  nM) (Fig. 5g).

In conclusion, these data indicate that EMO in general retain a comparable endometrial epithelial ion channel expression pattern as observed in hEEC, even over longer periods of culture. Moreover, the fingerprint of EMO for mechanosensitive ion channels is more comparable to the primary culture hEEC than the endometrial cancer HEC-1A cell line. However, both cellular models of endometrial epithelial cells showed reduced expression of *PIEZO1* compared to hEEC.

## Discussion

Studies assessing the underlying molecular mechanisms behind the embryo-uterine interplay are very scarce and molecular candidates involved in the early communication still need to be fully elucidated and characterized. Ion channels are potential candidates to govern signals and are emerging more often as important players in the field of reproductive medicine<sup>42,43</sup>. However, the fingerprint of ion channels in endometrial epithelial cells is very incomplete.



As the communication between blastocyst and epithelium can be both chemical and mechanical, the expression of mechanosensitive ion channels in endometrial epithelial cells of mouse and human was investigated. Importantly, mechanical stimulation of EEC resulted in robust  $\text{Ca}^{2+}$  influxes, and transient increases in current densities, that were not detected in the absence of extracellular  $\text{Ca}^{2+}$  and could be blocked in the presence of GsMTx4, an inhibitor of mechanosensitive channels. These results indicate for the first time the functional expression of one (or more) mechanosensitive ion channel(s) in endometrial epithelial cells of mouse and human. A first possible candidate is the PIEZO1 channel<sup>13</sup> since high mRNA-expression levels were detected in hEEC and in endometrial biopsies during different stages of the menstrual cycle. Similar expression results were detected in mouse that were supported by *in situ* hybridisation experiments showing positive staining for *Piezo1* RNA in EEC of the mouse uterine horn. Importantly, stimulation of EEC by the chemical agonist Yoda1 evoked robust  $\text{Ca}^{2+}$  influxes and resulted in an increase in current amplitudes in whole-cell patch clamp experiments. Corresponding results using mechanical and chemical activation, were obtained in HEK-293T cells overexpressing mouse PIEZO1, as previously demonstrated by several groups<sup>13,30,44</sup>, suggesting the functional expression of PIEZO1 as an endogenously expressed mechanosensitive ion channel in EEC of mouse and human. As homologous deletion of PIEZO1 in mice is embryonically lethal and *Piezo1*<sup>-/-</sup> pups die at mid gestation (E9.5–E11.5)<sup>45</sup>, the possibilities to gain further insights in the physiological role of PIEZO1 in the implantation process are limited and further research is necessary to underpin the role of PIEZO1 in embryo implantation.

Next, the expression of mechanosensitive  $\text{K}^+$  channels was investigated by RT-qPCR. However, the expression levels of *KCNK2* and *KCNK4* were below the detection limit in mouse and human cells, excluding them as a candidate mechanosensors in EEC. Moreover, additive experiments revealed mRNA expression of the mechanosensitive *TRPV1/V2/V4*, and *TRPC1/C4/C6* in hEEC. However,  $\text{Ca}^{2+}$ -microfluorimetric experiments showed no  $\text{Ca}^{2+}$  influx after stimulation with specific TRP channel agonists, indicating the lack of functional expression of these polymodal TRP channels. However, RT-qPCR studies and  $\text{Ca}^{2+}$  imaging experiments did indicate the functional expression of *TRPM7*, illustrating the correlation between RNA expression levels and functional protein expression in hEEC. The epithelial character of the endometrial cells was confirmed by the high mRNA expression of *ENaC* and the robust  $\text{Ca}^{2+}$  responses to trypsin stimulation. The trypsin-induced  $\text{Ca}^{2+}$  increase was assigned to the opening of voltage dependent calcium channels by an *ENaC*-induced membrane depolarization. This is in accordance with earlier studies describing a role for *ENaC* in triggering prostaglandin  $\text{E}_2$  production and release from the endometrial epithelium, required for embryo implantation<sup>12</sup>. Previous reports have described a role for *ENaC* in electrolyte and water reabsorption during the peri-implantation period in mice<sup>46</sup> and its function in the disappearance of uterine fluid, or the closure of the uterine lumen<sup>47</sup>. Although *ENaC* is described in some studies as a channel that can be activated by mechanical force<sup>10,11</sup>, several controversial results have been published on the mechanosensitivity of the channel<sup>48</sup>. Overall, these results provide strong evidence for the functional expression of PIEZO1 as mechanosensitive ion channel in the endometrial epithelial cells of human and mouse.

In addition, RT-qPCR experiments revealed mRNA expression of *TRPM4* and *TRPM7* in hEEC. Overall, the expression pattern of TRP channels in EEC is very limited and in strong contrast to the fingerprint that was observed in human endometrial stromal cells<sup>38</sup>. These results are in line with the distinct expression pattern of TRP channels described in endometrial epithelial and stromal cells in mouse. In mice, the overall expression of TRP channels in endometrial epithelial cells was very low, except for *Trpv4*, *Trpv6*, *Trpm4* and *Trpm6* that were significantly higher in epithelial cells as compared to stromal cells<sup>36</sup>. Remarkably, the gene expression of *TRPV4* and *TRPM6* in hEEC is situated around the detection level and thus lower as compared to the mouse expression pattern. These data are supported by the fact that no correlation could be detected in TRP channel expression pattern between mouse and human endometrial epithelial cells (Spearman correlation = 0.10;  $p = 0.746$ ) (Supplementary Fig. S10). Stimulation with a *TRPV4* agonist did not induce any  $\text{Ca}^{2+}$  influx, indicating no functional expression of *TRPV4* in human. This outcome is in contrast with mouse EEC where stimulation by GSK induced robust  $\text{Ca}^{2+}$  influxes which could be blocked by the *TRPV4* inhibitor HC067047<sup>36</sup>. This discrepancy between mouse and human could be explained as a species difference. Alternatively, there could be a difference in origin of the epithelial cells, since it is currently unclear whether luminal epithelial cells share a similar expression pattern compared to the glandular epithelial cells. Most probably, the primary culture of mouse EEC originates from the luminal epithelial, whereas the origin of human EEC is unclear. Or else, it is possible that a difference in culture conditions between mouse (1–2 days in culture) and human EEC (2–4 days) induces changes in the expression levels. In addition, *TRPV6* gene expression levels were significant in both mouse and human epithelial cells as visualized by *in situ* hybridization studies in mouse, and could suggest an important role for *TRPV6* in the embryo implantation process. Indeed, female mice lacking functional *TRPV6* are sub-fertile, showed an increased latency to pregnancy and displayed a smaller litter size<sup>49</sup>. Nonetheless, *TRPV6* expression was lower in human cells compared to mouse. Since *TRPV6* expression in the Ishikawa cell line is upregulated by  $\text{E}_2$ , the increased *Trpv6* levels in mouse EEC could be explained by the difference in isolation protocol in which the animals are treated by high doses of  $\text{E}_2$ <sup>50</sup>.

Unravelling the paracrine signalling between the blastocyst and the endometrium *in vitro* is often restricted as obtaining, isolating and culturing hEEC has proven challenging. Alternatively, many groups resort to endometrial epithelial cell lines, such as HEC-1A, Ishikawa cells, ECC-1, RL95-2, and others to overcome this problem. Most of these cell lines are established from endometrial adenocarcinomas several decades ago and have distinct properties in terms of adhesiveness and the presence of hormones, receptors and adhesion molecules<sup>41,51,52</sup>. Moreover, aside from their cancer profile, it has been shown that the long-term culture and use of these cell lines can result in loss of integrity and genetic changes<sup>51,53</sup>. Recently, endometrial epithelial organoids (EMO) have been proposed as an alternative research tool in implantation studies<sup>25,40</sup>. The EMO are derived from endometrial biopsies, but exhibit the advantage to be established from limited amounts of starting material, expanded into high cell yields and kept in culture for long periods of time. The organoids phenocopy physiological responses of the endometrial epithelium to hormones and can replicate the menstrual cycle under hormonal treatment<sup>25</sup>. In addition, when

seeded on standard culture plates, EMO-derived cells establish a 2D monolayer that resembles the morphology of hEEC. Together, these characteristics make organoids more appealing to use in *in vitro* studies. This study has evaluated the expression pattern of ion channels in EMO and compared this fingerprint to primary hEEC. Overall, these results showed corresponding functional expression patterns of mechanosensitive and TRP channels between hEEC and EMO, although there may be a tendency of lower expression levels in EMO. A plausible explanation could be the difference in culture conditions: whereas hEEC are cultured in the presence of serum, the organoids are expanded in serum-free medium. Moreover, the organoids are cultured in the presence of estradiol which makes them representative of the proliferative phase of the menstrual cycle<sup>25</sup>. Alternatively, the potential significance in expression pattern can be due to the fact that the biopsies are isolated from patients undergoing fertility treatment and might have an altered expression pattern. In addition, the origin of the epithelial cells in EMO is not known and may differ from the origin of the hEEC. Nevertheless, the TRP channel expression pattern of hEEC showed a positive correlation compared to EMO (Spearman correlation = 0.66;  $p < 0.05$ ). Intriguingly, expression of the *PIEZO1* channel was not detected in 3D organoids, but mechanical stimulation of the cell membrane by poking or application of a hypotonic solution and ligand stimulation resulted in  $Ca^{2+}$  influxes in the organoid-derived 2D cultures, suggesting that expression was restored. Indeed, RT-qPCR results on 2D and 3D cultures of organoids showed increased *PIEZO1* RNA expression upon 2D culture conditions. The effect of 3D culture on mechanical transduction and signalling has already been illustrated<sup>54</sup> and therefore, the altered cell conformation may have induced an upregulation of *PIEZO1*, independent of FBS supplementation to the culture medium.

Further, the effect of long-term expandability of EMO was investigated by evaluating the expression of a selected panel of ion channels in early (P2) and late passage long-term EMO culture (P8). Overall, no significant differences were noticed between early and late passages for gene- and functional expression, supporting the stable character of the EMO.

Finally, the expression pattern of hEEC and EMO for mechanosensitive ion channels was further compared to that of the endometrial cancer cell line HEC-1A. In general, these results showed a very low expression of ion channels in HEC-1A cells, even the expression of the epithelial marker *TRPV6* was below the detection level. Moreover, no correlation was observed between the expression pattern of ion channels between hEEC and HEC-1A. Mechanical and ligand stimulation of HEC-1A cells induced influxes in intracellular  $Ca^{2+}$  concentration, indicating the presence of functional *PIEZO1*. However, the sensitivity of HEC-1A cells towards mechanical stimulation was significantly reduced compared to EMO as illustrated by the increased indentation necessary to evoke a  $Ca^{2+}$  influx and the reduced response to application of a HTS. Moreover, HEC-1A cells displayed significantly larger  $Ca^{2+}$  influxes towards trypsin stimulation compared to hEEC and EMO (Fig. 5g). This modified response towards trypsin stimulation can be explained by an altered expression pattern of other proteins involved in the influx or release of  $Ca^{2+}$ . Since trypsin is a non-selective agonist, it cannot be excluded that this stimulus acts on different proteins involved in inducing an increase in  $Ca^{2+}$  concentration. An altered gene-expression could also explain the carcinogenic character of the HEC-1A cells and their ability to survive long-term culture. Overall, these data argue that EMO are a more representative *in vitro* model to study mechanosensitive ion channels in implantation compared to HEC-1A cells that are derived from an endometrial adenocarcinoma obtained from a patient of non-reproductive age<sup>55</sup>. In contrast, primary EMO are obtained from control tissue at reproductive age and closely replicate the endometrial epithelium in terms of expression of specific markers, mucus production, responsiveness to regulatory hormones and simulation of the human menstrual cycle<sup>25</sup>.

Altogether, these experiments validate for endometrial organoids as a representative model for primary EEC and provide further support for the use of EMO as an *in vitro* model to study interactions between the blastocyst and the endometrial epithelium.

In conclusion, this research concentrates on the expression of mechanosensitive ion channels in EEC that might be crucial in the embryo-uterine crosstalk. Our results provide strong evidence for the functional expression of *PIEZO1* in EEC of mouse and human, suggesting a potential role as signal transducer in embryo implantation. Additionally, we showed a specific expression pattern of TRP channels in hEEC, which is distinct from the earlier described expression in endometrial stromal cells. Finally, our results validate endometrial organoids as a solid *in vitro* implantation model to examine the role of mechanosensitive ion channels in embryo implantation.

## Methods

**Sample collection.** *Ethical approval.* All samples were collected at the Leuven University Fertility Centre with the approval of the Ethical Committee of the University Hospital Gasthuisberg, Leuven, Belgium (S54776, S60959 and S59006) and after written informed consent of the patient. By signing the informed consent patients agreed to publish obtained results. All research was performed accordance the approved guidelines and regulations.

*Collection of human endometrial biopsies.* Endometrial biopsies were obtained from patients of reproductive age who underwent the procedure as part of the diagnostic examination in their fertility treatment. Endometrial biopsies were taken using a sterile pipelle canulla or Novak curette.

For the isolation of primary EEC, biopsies were obtained from patients who were in the luteal phase of their menstrual cycle free of any hormonal medication prior to the procedure.

**Cell culture.** *Isolation of primary human endometrial epithelial cells.* The protocol used is based on previously described methods<sup>56–58</sup>.

Immediately after the collection of the endometrial biopsy, the tissue was rinsed with phosphate buffered saline (PBS) to remove all blood and mucus. The biopsy was minced into 1 mm<sup>2</sup> pieces and incubated in phenol-red free, low glucose DMEM supplemented with 1 mg/ml collagenase type I (Sigma-Aldrich, Belgium)

for 60 min at 37 °C on a shaker, or overnight at 4 °C. After incubation, the resultant cell mixture was shaken thoroughly and poured through a 20 µm cell strainer. The filtrate containing the endometrial stromal cells (hESC) was centrifuged for 5 min at 720 × g, resuspended in growth medium containing DMEM/F12 supplemented with 10% fetal bovine serum (FBS), 0.2% gentamycin and 0.2% amphotericin B, and seeded in the appropriate wells, whereas the EEC were retained by the strainer. The epithelial fraction was collected by backwashing the cell strainer with growth medium consisting of phenol-red free, low glucose DMEM, 10% FBS, 20% MCDB-105, 5 µg/ml insulin, 0.2% gentamycin and 0.2% amphotericin B. The flow-through was mechanically disrupted by gently pipetting the solution up and down, collected in a T75 flask and incubated for a minimum of 30 min at 37 °C in 5% CO<sub>2</sub>. After incubation, the cells were collected, centrifuged at 720 × g, resuspended in growth medium and seeded in the appropriate cell culture plates for further experiments. Cells were kept at 37 °C in 5% CO<sub>2</sub> and the medium was changed every 2 days. All experiments were performed on EEC at P0.

**Isolation of primary mouse endometrial epithelial cells.** Primary mEEC and mESC cells were isolated as previously described<sup>32</sup>. The use of mice for these experiments was approved by the ethical committee for animal experiments and welfare of the KU Leuven (p102/2017). All experiments were performed according to the approved guidelines and regulations.

**Human endometrial organoids.** Human endometrial organoids (EMO) were generated as previously described by Boretto *et al.*<sup>25</sup>. Endometrial biopsies were obtained from hormonally non-treated patients undergoing laparoscopy for benign gynecological conditions. All experiments were performed with EMO of early passage (P1-3) or late passage (P8).

**Culture of HEC-1A and HEK-293T cells.** The HEC-1A endometrial adenocarcinoma cell line was kindly provided by F. Vilella and C. Simón and cultured using growth medium consisting of McCoys 5A modified medium, 10% FBS, 0.2% gentamycin and 0.2% amphotericin B. HEK-293T cells were cultured as previously described<sup>59</sup>, and transiently transfected with 2 µg of murine *Piezo1* cDNA construct (kindly provided by A. Patapoutian) using Mirus TranIT-293 transfection reagent (Mirus Corporation, USA) 72 hrs before measurements. Transfected cells were visualized by green fluorescence protein (GFP) expression. GFP-negative cells from the same batch were used as controls.

**Immunocytochemistry.** Human EEC were seeded in a 12-well plate on collagen-coated (Sigma-Aldrich, Belgium) coverslips (Karl Hecht, Germany). The growth medium was removed and cells were fixed with a 1:1 mixture of EtOH and 4% paraformaldehyde for 1 min, permeabilized with 0.25% Triton X-100 for 10 min, and blocked with 3% normal goat serum for 15 min. The primary monoclonal antibody mouse anti-human MMP-2 (0.5 µg/ml; 1/200) (Abcam, United Kingdom) or polyclonal rabbit anti-human MMP-7 (0.5 µg/ml; 1/40) (Abcam) was incubated overnight at 4 °C. The cells were further incubated for 1 h with horseradish peroxidase-labelled secondary goat anti-rabbit or goat anti-mouse antibodies (1/100, EnVision system) (Agilent, Belgium). The substrate was stained with diaminobenzidine (DAB) (Sigma Aldrich, Belgium) and counterstained with Mayer Haematoxyline.

**RNAscope *in situ* hybridization assay.** The RNAscope Multiplex Fluorescent Reagent Kit (Advanced Cell Diagnostics, US) was used for the *in situ* hybridization (ISH) of *Piezo1* in mouse uterus, bladder and trigeminal neurons. The ISH assay was performed according to the manufacturers' guidelines for formalin-fixed, paraffin-embedded samples. In brief, tissue samples were pre-treated via the application of RNAscope hydrogen peroxide and Protease IV. Murine *Piezo1* or *Trpv6* specific probe (Advanced Cell Diagnostics, US) was applied for 2 h at 40 °C in a HybEZ oven. Samples were washed, and signal amplification steps were carried out. The signal was detected using fluorescently labelled probes and sections were incubated with DAPI.

**RNA extraction and RT-qPCR.** Total RNA from hEEC and endometrial cell lines was isolated, after 2–4 days of culture, using the RNeasy Mini kit (Qiagen, The Netherlands). For the EMO, the RNeasy Micro kit (Qiagen, The Netherlands) was used. RNA was isolated according to the manufacturers' guidelines. RNA concentration and quality were assessed via the Nanodrop method (Isogen Life Science, Belgium) and Experion RNA Analysis kit (Bio-Rad, Belgium). cDNA was generated from 1 µg of RNA using the First-Strand cDNA Synthesis Kit (GE Healthcare, Belgium). RT-qPCR was performed on triplicate cDNA samples using specific TaqMan gene expression assays (Supplementary Table I) (Life Technologies, Belgium) in the StepOne PCR system (Applied Biosystems, Belgium). Hypoxanthine Phosphoribosyltransferase 1 (*HPRT1*) and Phosphoglycerate Kinase 1 (*PGK1*) were used as endogenous controls. Data is represented as mean ± SEM of  $2^{(-\Delta Ct)}$  for which  $\Delta Ct = C_{t_{\text{gene of interest}}} - C_{t_{\text{geometric mean of HPRT1 and PGK1}}}$ .

**Functional measurements.** **Pharmacology.** Functional PIEZO1 and ENaC activity was evaluated using 5 µM 2-[5-[[[(2,6-Dichlorophenyl)methyl]thio]-1,3,4-thiadiazol-2-yl]pyrazine (Yoda1) (Interchim, France) and 2 µg/ml trypsin respectively. *Grammostola spatulata* mechanotoxin 4 (GsMTx4, 20 µM) (Alomone Labs, Israel) was used to challenge mechanically induced responses. TRP channel responses were measured using 50 µM  $\Delta^9$ -tetrahydrocannabinol (THC) for TRPV2, 10 nM GSK1016790A (GSK) (Sigma-Aldrich, Belgium) for TRPV4, 250 nM (–) Englerin A (EA) (Phytolabs, Germany) for TRPC1/4, 100 µM 1-oleoyl-2-acetyl-glycerol (OAG) (Calbiochem, The Netherlands) for TRPC6, and 200 µM mibefradil (Mib) (Sigma-Aldrich, Belgium) for TRPM7. HC-067047 (HC, 100 nM) (Sigma-Aldrich, Belgium) was used to challenge TRPV4-induced responses. 2 µM ionomycin was applied as positive control at the end of each experiment. All stock solutions were prepared in either DMSO, Milli Q water or EtOH.

**Calcium imaging.** The measurement of intracellular  $\text{Ca}^{2+}$  was performed as previously described<sup>36</sup>. Absolute calcium concentrations were calculated from the ratio of the fluorescence signals at both wavelengths (F340/F380) after correction for the individual background fluorescence signals, using the Grynkiewicz equation<sup>60</sup>:

$$[\text{Ca}^{2+}] = K_{\text{eff}} \frac{R - R_0}{R_1 - R}$$

where the calibration constants  $R_0$ ,  $R_1$  and  $K_{\text{eff}}$  were determined as followed:  $R_0$  defines the ratio in  $\text{Ca}^{2+}$  free medium supplemented with 10 mM EGTA, whereas  $R_1$  comprises the ratio in high  $\text{Ca}^{2+}$  medium (10 mM).  $K_{\text{eff}}$ , the effective binding constant, includes  $R_0$ ,  $R_1$ , the dissociation constant of indicator dye  $K_D$ , and the isocoefficient  $\alpha$ , according to the following equation:

$$K_{\text{eff}} = K_D \frac{R_1 + \alpha}{R_0 + \alpha}$$

The  $K_D$  of Fura-2 and the isocoefficient  $\alpha$  were assumed as described by Zhou and Neher<sup>61</sup>.

Cells were considered responders if the amplitude of the rise in intracellular calcium during agonist application exceeded 100 nM and when the highest value of the derivative of the calcium trace during the application of an activator exceeded at least 3 times the standard deviation of the derivative during basal conditions. Calcium amplitudes were calculated as the difference between the maximum calcium and basal calcium of responding cells during the application of an activator. Only cells that responded to the positive control, ionomycin, at the end of the experiment were taken into account. For all measurements, the following bath solution was used (in mM): 150 NaCl, 2  $\text{CaCl}_2$ , 1  $\text{MgCl}_2$ , 10 D-glucose and 10 HEPES (pH 7.4 with NaOH). For measuring the swelling-activated calcium influx, an isotonic solution was used containing (in mM): 105 NaCl, 6  $\text{CsCl}_2$ , 5  $\text{CaCl}_2$ , 1  $\text{MgCl}_2$ , 10 D-glucose, 10 HEPES and 90 D-mannitol, pH 7.4 with NaOH (320 milliosmolar). Cell swelling was induced by omitting mannitol from this solution, and reducing NaCl to 80 mM (giving 210 milliosmolar). The measurements under calcium-free conditions were performed with similar solutions in which 5 mM  $\text{CaCl}_2$  was omitted and replaced with 5 mM EDTA. All experiments were performed in triplicate ( $n \geq 3$ ) on at least 80 cells.

**Mechanical stimulation of cells.** Mechanical stimulation was applied via a glass probe using the E-625 piezo controller (Physik Instrumente, Germany) with computer interface and interpreter. Calcium signals were evaluated after incubation of the cells with 2  $\mu\text{M}$  Fura-2 acetoxymethyl ester for 30 min at 37 °C. The fluorescent signal was detected during alternating illumination between 340 and 380 nm on a Cell<sup>M</sup> fluorescence microscope (Olympus, USA). The ratio of the fluorescence values at the two wavelengths (F340/F380) was determined after correction for the individual background signals. The absolute intracellular calcium values were calculated from the fluorescence ratios using the Grynkiewicz equation as described above<sup>60</sup>. For all measurements, the following bath solution was used (in mM): 150 NaCl, 2  $\text{CaCl}_2$ , 1  $\text{MgCl}_2$ , 10 D-glucose and 10 HEPES (pH 7.4 with NaOH).

**Whole-cell patch clamp.** Whole-cell patch clamp recordings were measured with an EPC-10 amplifier and the PatchMasterPro Software (HEKA Elektronik, Lambrecht, Germany). Current measurements were performed at a sampling rate of 20 kHz and currents were digitally filtered at 2.9 kHz. In all measurements, 70% of the series resistance was compensated. The standard internal solution contained (in mM): 100 Asp, 45 CsCl, 10 EGTA, 10 HEPES, 1  $\text{MgCl}_2$  (pH 7.2 with CsOH) and the standard extracellular solution contained (in mM): 150 NaCl, 10 HEPES, 10 Glucose, 2  $\text{CaCl}_2$ , 1  $\text{MgCl}_2$  (pH 7.4 with NaOH). The standard patch pipette resistance was between 2 M $\Omega$  and 4 M $\Omega$  when filled with pipette solution.

**Data and statistical analysis.**  $\text{Ca}^{2+}$  microfluorimetric and electrophysiological data were analyzed using home-written routines in IgorPro 6.37 (WaveMetrics, USA), and OriginPro 9 (OriginLab Corporation, USA) was further used for data display. Statistical analysis was conducted via GraphPad Prism version 7.04 (GraphPad Software, USA).

## Data Availability

The datasets generated during the current study are available from the corresponding author upon reasonable request.

## References

- Norwitz, E. R., Schust, D. J. & Fisher, S. J. Implantation and the survival of early pregnancy. *N Engl J Med* **345**, 1400–1408, <https://doi.org/10.1056/NEJMra000763> (2001).
- Wilcox, A. J. *et al.* Incidence of early loss of pregnancy. *N Engl J Med* **319**, 189–194, <https://doi.org/10.1056/NEJM198807283190401> (1988).
- Brosens, J. J. *et al.* Uterine selection of human embryos at implantation. *Scientific reports* **4**, 3894, <https://doi.org/10.1038/srep03894> (2014).
- Enders, A. C., Given, R. L. & Schlafke, S. Differentiation and migration of endoderm in the rat and mouse at implantation. *Anat Rec* **190**, 65–77, <https://doi.org/10.1002/ar.1091900107> (1978).
- Lejeune, B., Lecocq, R., Lamy, F. & Leroy, F. Changes in the pattern of endometrial protein synthesis during decidualization in the rat. *J Reprod Fertil* **66**, 519–523 (1982).
- Lejeune, B., Van Hoeck, J. & Leroy, F. Transmitter role of the luminal uterine epithelium in the induction of decidualization in rats. *J Reprod Fertil* **61**, 235–240 (1981).
- Almog, B., Shalom-Paz, E., Dufort, D. & Tulandi, T. Promoting implantation by local injury to the endometrium. *Fertility and sterility* **94**, 2026–2029, <https://doi.org/10.1016/j.fertnstert.2009.12.075> (2010).



8. Nastro, C. O. *et al.* Endometrial injury in women undergoing assisted reproductive techniques. *The Cochrane database of systematic reviews* 3, CD009517, <https://doi.org/10.1002/14651858.CD009517.pub3> (2015).
9. Potdar, N., Gelbaya, T. & Nardo, L. G. Endometrial injury to overcome recurrent embryo implantation failure: a systematic review and meta-analysis. *Reprod Biomed Online* 25, 561–571, <https://doi.org/10.1016/j.rbmo.2012.08.005> (2012).
10. Fronius, M. & Clauss, W. G. Mechano-sensitivity of ENaC: may the (shear) force be with you. *Pflugers Archiv: European journal of physiology* 455, 775–785, <https://doi.org/10.1007/s00424-007-0332-1> (2008).
11. Simon, A., Shenton, F., Hunter, I., Banks, R. W. & Bewick, G. S. Amiloride-sensitive channels are a major contributor to mechanotransduction in mammalian muscle spindles. *J Physiol* 588, 171–185, <https://doi.org/10.1113/jphysiol.2009.182683> (2010).
12. Ruan, Y. C. *et al.* Activation of the epithelial Na<sup>+</sup> channel triggers prostaglandin E<sub>2</sub> release and production required for embryo implantation. *Nature medicine* 18, 1112–1117, <https://doi.org/10.1038/nm.2771> (2012).
13. Coste, B. *et al.* Piezo1 and Piezo2 are essential components of distinct mechanically activated cation channels. *Science* 330, 55–60, <https://doi.org/10.1126/science.1193270> (2010).
14. Alessandri-Haber, N. *et al.* Hypotonicity induces TRPV4-mediated nociception in rat. *Neuron* 39, 497–511 (2003).
15. Servin-Vences, M. R., Moroni, M., Lewin, G. R. & Poole, K. Direct measurement of TRPV4 and PIEZO1 activity reveals multiple mechanotransduction pathways in chondrocytes. *Elife* 6, <https://doi.org/10.7554/eLife.21074> (2017).
16. Oancea, E., Wolfe, J. T. & Clapham, D. E. Functional TRPM7 channels accumulate at the plasma membrane in response to fluid flow. *Circulation research* 98, 245–253, <https://doi.org/10.1161/01.RES.0000200179.29375.cc> (2006).
17. Vriens, J. *et al.* Cell swelling, heat, and chemical agonists use distinct pathways for the activation of the cation channel TRPV4. *Proceedings of the National Academy of Sciences of the United States of America* 101, 396–401, <https://doi.org/10.1073/pnas.030329101> (2004).
18. Numata, T., Shimizu, T. & Okada, Y. TRPM7 is a stretch- and swelling-activated cation channel involved in volume regulation in human epithelial cells. *American journal of physiology. Cell physiology* 292, C460–467, <https://doi.org/10.1152/ajpcell.00367.2006> (2007).
19. Liedtke, W. *et al.* Vanilloid receptor-related osmotically activated channel (VR-OAC), a candidate vertebrate osmoreceptor. *Cell* 103, 525–535 (2000).
20. Strotmann, R., Harteneck, C., Nunnenmacher, K., Schultz, G. & Plant, T. D. OTRPC4, a nonselective cation channel that confers sensitivity to extracellular osmolarity. *Nat Cell Biol* 2, 695–702, <https://doi.org/10.1038/35036318> (2000).
21. Muraki, K. *et al.* TRPV2 is a component of osmotically sensitive cation channels in murine aortic myocytes. *Circulation research* 93, 829–838, <https://doi.org/10.1161/01.RES.0000097263.10220.0C> (2003).
22. Ciura, S. & Bourque, C. W. Transient receptor potential vanilloid 1 is required for intrinsic osmoreception in organum vasculosum lamina terminalis neurons and for normal thirst responses to systemic hyperosmolality. *J Neurosci* 26, 9069–9075, <https://doi.org/10.1523/JNEUROSCI.0877-06.2006> (2006).
23. Wissenbach, U., Boddling, M., Freichel, M. & Flockerzi, V. Trp12, a novel Trp related protein from kidney. *FEBS Lett* 485, 127–134 (2000).
24. Hannan, N. J., Paiva, P., Dimitriadis, E. & Salamonsen, L. A. Models for study of human embryo implantation: choice of cell lines? *Biol Reprod* 82, 235–245, <https://doi.org/10.1095/biolreprod.109.077800> (2010).
25. Boretto, M. *et al.* Development of organoids from mouse and human endometrium showing endometrial epithelium physiology and long-term expandability. *Development* 144, 1775–1786, <https://doi.org/10.1242/dev.148478> (2017).
26. Matsuzaki, S., Maleysson, E. & Darcha, C. Analysis of matrix metalloproteinase-7 expression in eutopic and ectopic endometrium samples from patients with different forms of endometriosis. *Hum Reprod* 25, 742–750, <https://doi.org/10.1093/humrep/dep435> (2010).
27. Bae, C., Sachs, F. & Gottlieb, P. A. The mechanosensitive ion channel Piezo1 is inhibited by the peptide GsMTx4. *Biochemistry* 50, 6295–6300, <https://doi.org/10.1021/bi200770q> (2011).
28. Maingret, F., Fosset, M., Lesage, F., Lazdunski, M. & Honore, E. TRAAK is a mammalian neuronal mechano-gated K<sup>+</sup> channel. *J Biol Chem* 274, 1381–1387 (1999).
29. Patel, A. J. *et al.* A mammalian two pore domain mechano-gated S-like K<sup>+</sup> channel. *EMBO J* 17, 4283–4290, <https://doi.org/10.1093/emboj/17.15.4283> (1998).
30. Syeda, R. *et al.* Chemical activation of the mechanotransduction channel Piezo1. *Elife* 4, <https://doi.org/10.7554/eLife.07369> (2015).
31. Vallet, V., Chraïbi, A., Gaeggeler, H. P., Horisberger, J. D. & Rossier, B. C. An epithelial serine protease activates the amiloride-sensitive sodium channel. *Nature* 389, 607–610, <https://doi.org/10.1038/39329> (1997).
32. De Clercq, K., Hennes, A. & Vriens, J. *In vitro* decidualization in a coculture of mouse endometrial epithelial and stromal cells. *JoVe* In press.
33. Everaerts, W. *et al.* Inhibition of the cation channel TRPV4 improves bladder function in mice and rats with cyclophosphamide-induced cystitis. *Proceedings of the National Academy of Sciences of the United States of America* 107, 19084–19089, <https://doi.org/10.1073/pnas.1005333107> (2010).
34. Gottlieb, P. A., Bae, C. & Sachs, F. Gating the mechanical channel Piezo1: a comparison between whole-cell and patch recording. *Channels (Austin)* 6, 282–289, <https://doi.org/10.4161/chan.21064> (2012).
35. Miyamoto, T. *et al.* Functional role for Piezo1 in stretch-evoked Ca<sup>2+</sup>(+) influx and ATP release in urothelial cell cultures. *The Journal of biological chemistry* 289, 16565–16575, <https://doi.org/10.1074/jbc.M113.528638> (2014).
36. De Clercq, K. *et al.* The functional expression of transient receptor potential channels in the mouse endometrium. *Hum Reprod* 32, 615–630, <https://doi.org/10.1093/humrep/dew344> (2017).
37. Gomis, A. In *TRP Channels in Sensory Transduction* (eds Rodolfo Madrid & Juan Bacigalupo) 141–163 (Springer International Publishing, 2015).
38. De Clercq, K. *et al.* Functional expression of transient receptor potential channels in human endometrial stromal cells during the luteal phase of the menstrual cycle. *Hum Reprod* 30, 1421–1436, <https://doi.org/10.1093/humrep/dev068> (2015).
39. Schafer, S. *et al.* Mibefradil represents a new class of benzimidazole TRPM7 channel agonists. *Pflugers Archiv: European journal of physiology* 468, 623–634, <https://doi.org/10.1007/s00424-015-1772-7> (2016).
40. Turco, M. Y. *et al.* Long-term, hormone-responsive organoid cultures of human endometrium in a chemically defined medium. *Nat Cell Biol* 19, 568–577, <https://doi.org/10.1038/ncb3516> (2017).
41. Kuramoto, H., Tamura, S. & Notake, Y. Establishment of a cell line of human endometrial adenocarcinoma *in vitro*. *Am J Obstet Gynecol* 114, 1012–1019 (1972).
42. Ruan, Y. C., Chen, H. & Chan, H. C. Ion channels in the endometrium: regulation of endometrial receptivity and embryo implantation. *Human reproduction update* 20, 517–529, <https://doi.org/10.1093/humupd/dmu006> (2014).
43. Jing, C. *et al.* TRPC3 Overexpression Promotes the Progression of Inflammation-Induced Preterm Labor and Inhibits T Cell Activation. *Cell Physiol Biochem* 45, 378–388, <https://doi.org/10.1159/000486912> (2018).
44. Lewis, A. H. & Grandl, J. Mechanical sensitivity of Piezo1 ion channels can be tuned by cellular membrane tension. *Elife* 4, <https://doi.org/10.7554/eLife.12088> (2015).
45. Li, J. *et al.* Piezo1 integration of vascular architecture with physiological force. *Nature* 515, 279–282, <https://doi.org/10.1038/nature13701> (2014).
46. Kellenberger, S. & Schild, L. Epithelial sodium channel/degenerin family of ion channels: a variety of functions for a shared structure. *Physiological reviews* 82, 735–767, <https://doi.org/10.1152/physrev.00007.2002> (2002).



47. Yang, J. Z. *et al.* Differential expression and localization of CFTR and ENaC in mouse endometrium during pre-implantation. *Cell Biol Int* **28**, 433–439, <https://doi.org/10.1016/j.cellbi.2004.03.011> (2004).
48. Rusch, A. & Hummler, E. Mechano-electrical transduction in mice lacking the alpha-subunit of the epithelial sodium channel. *Hear Res* **131**, 170–176 (1999).
49. Bianco, S. D. *et al.* Marked disturbance of calcium homeostasis in mice with targeted disruption of the Trpv6 calcium channel gene. *J Bone Miner Res* **22**, 274–285, <https://doi.org/10.1359/jbmr.061110> (2007).
50. Yang, H., Choi, K. C., Hyun, S. H. & Jeung, E. B. Coexpression and estrogen-mediated regulation of TRPV6 and PMCA1 in the human endometrium during the menstrual cycle. *Mol Reprod Dev* **78**, 274–282, <https://doi.org/10.1002/mrd.21303> (2011).
51. Nishida, M. The Ishikawa cells from birth to the present. *Hum Cell* **15**, 104–117 (2002).
52. Way, D. L., Grosso, D. S., Davis, J. R., Surwit, E. A. & Christian, C. D. Characterization of a new human endometrial carcinoma (RL95-2) established in tissue culture. *In Vitro* **19**, 147–158 (1983).
53. Korch, C. *et al.* DNA profiling analysis of endometrial and ovarian cell lines reveals misidentification, redundancy and contamination. *Gynecol Oncol* **127**, 241–248, <https://doi.org/10.1016/j.ygyno.2012.06.017> (2012).
54. Baker, B. M. & Chen, C. S. Deconstructing the third dimension: how 3D culture microenvironments alter cellular cues. *J Cell Sci* **125**, 3015–3024, <https://doi.org/10.1242/jcs.079509> (2012).
55. HEC-1-A (CVCL\_0293), [https://web.expasy.org/cellosaurus/CVCL\\_0293](https://web.expasy.org/cellosaurus/CVCL_0293) (ExPASy - Bioinformatics Research Portal).
56. Masuda, A. *et al.* An improved method for isolation of epithelial and stromal cells from the human endometrium. *J Reprod Dev* **62**, 213–218, <https://doi.org/10.1262/jrd.2015-137> (2016).
57. Simón, C. *et al.* Embryonic regulation of integrins beta 3, alpha 4, and alpha 1 in human endometrial epithelial cells *in vitro*. *The Journal of clinical endocrinology and metabolism* **82**, 2607–2616, <https://doi.org/10.1210/jcem.82.8.4153> (1997).
58. Chen, J. C. & Roan, N. R. Isolation and Culture of Human Endometrial Epithelial Cells and Stromal Fibroblasts. *Bio Protoc* **5** (2015).
59. Vriens, J. *et al.* TRPM3 is a nociceptor channel involved in the detection of noxious heat. *Neuron* **70**, 482–494, <https://doi.org/10.1016/j.neuron.2011.02.051> (2011).
60. Grynkiewicz, G., Poenie, M. & Tsien, R. Y. A new generation of Ca<sup>2+</sup> indicators with greatly improved fluorescence properties. *J Biol Chem* **260**, 3440–3450 (1985).
61. Zhou, Z. & Neher, E. Mobile and immobile calcium buffers in bovine adrenal chromaffin cells. *J Physiol* **469**, 245–273 (1993).

## Acknowledgements

We thank all members of the Laboratory of Endometrium, Endometriosis and Reproductive Medicine (LEERM) and the members of the Laboratory of Ion Channel Research (LICR) of the KU Leuven, Leuven, Belgium for their experimental help and constructive discussions. We thank the health care personnel of the Leuven University Fertility Centre for the help in tissue acquisition. We are very grateful to Prof G. Appendino for providing us with chemical compounds, and to Prof A. Patapoutian for the donation of the mouse *Piezo1* construct.

## Author Contributions

A.H. is responsible for the development of concept and design, performing experiments, analysing and interpreting data, generation of figures and writing of the manuscript. K.H. performed electrophysiological experiments, analysed data and assisted in the generation of the figures. M.B. cultured and provided the endometrial organoids, contributed to the conceptual input for the organoid studies and revised the article critically for important intellectual content. K.D.C. and C.V.D.E. assisted in data collection and revised the article critically for important intellectual content. N.V.R., C.L. and Me.B. assisted with cellular or molecular experiments. A.V., K.P., C.T. and C.M. contributed to the acquisition of samples and revision of the article for important intellectual content. T.V. and H.V. assisted in acquisition and interpretation of data, and critically revised the article for important intellectual content. J.V. contributed to the concept and design, performing experiments, analysing data, interpretation of data, generation of figures, writing and revision of the article. All authors gave approval for the final version to be published.

## Additional Information

**Supplementary information** accompanies this paper at <https://doi.org/10.1038/s41598-018-38376-8>.

**Competing Interests:** The authors declare no competing interests.

**Publisher's note:** Springer Nature remains neutral with regard to jurisdictional claims in published maps and institutional affiliations.



**Open Access** This article is licensed under a Creative Commons Attribution 4.0 International License, which permits use, sharing, adaptation, distribution and reproduction in any medium or format, as long as you give appropriate credit to the original author(s) and the source, provide a link to the Creative Commons license, and indicate if changes were made. The images or other third party material in this article are included in the article's Creative Commons license, unless indicated otherwise in a credit line to the material. If material is not included in the article's Creative Commons license and your intended use is not permitted by statutory regulation or exceeds the permitted use, you will need to obtain permission directly from the copyright holder. To view a copy of this license, visit <http://creativecommons.org/licenses/by/4.0/>.

© The Author(s) 2019